Original Paper *Forma*, **26**, 19–24, 2011

A 4D Model Generator of the Human Lung

Hiroko Kitaoka

Division of Engineering Technology, JSOL Corporation, Marunouchi 2-18-25, Naka-ku, Nagoya 460-0002, Japan
E-mail address: hirokokitaoka000@hotmail.com

(Received April 16, 2011; Accepted July 13, 2011)

The present author has developed a free application software which generates 4D (=3D space + time) models of the human lung for the purpose of studying respiratory anatomy and physiology. The model generator makes air pathway models from the trachea to alveoli based on four algorithms published previously. An algorithm which converts geometric models into 4D finite element models is included in the software. According to user's interest and available computer resource, various model types can be selected such as airway tree, lung lobe, pulmonary acinus, and alveolar duct. The present author has also developed Origami models for the alveolar duct nearly equivalent to the computer models so that users may handle them in reality. The model generator will be a powerful tool for studying 4D respirology.

Key words: Broncho-Alveolar System, Dynamic Model, 4D, Software, Origami

1. Introduction

Anatomy and physiology are basic and traditional disciplines of medical science, which treat structures and functions of living organs, respectively. From a mathematical point of view, structure is a spatial arrangement of elements of which the organ consists, and the function is temporal differentiation of the structure. For example, the heart transports blood by changing spatial arrangements of myocardial fibers periodically. Likewise, the lung transports air by changing spatial arrangements of the parenchymal tissue periodically. At the molecular level, a functional molecule changes its conformation within a biological cycle. Signal transduction at the cell level is a compound phenomenon of mass transfer and conformation change of multiple molecules. Therefore, the living system should ideally be described as a 4D (3D space + time) object which includes structure, function, and the relationship between them.

Regarding the lung, conventional respiratory physiology uses analogy of tube-balloon combination for ventilation mechanics, in which the lung parenchyma, consisting of several hundred millions of alveoli, is replaced by one or a few number of empty air bags. However, this analogy is too simple to explain intrapulmonary ventilation distribution. In order to study "intrapulmonary" respiratory physiology, 4D models of the intrapulmonary structure are necessary. The present author has developed a free application software which generates various kinds of 4D lung models based on four algorithms previously published (Kitaoka *et al.*, 1999, 2000, 2007; Kitaoka and Kawase, 2007). An algorithm which converts geometric models into 4D finite element models for airflow simulation by computational fluid dynamics (CFD) was developed (Kitaoka, 2009), and is included in the resent software. Generated models are visualized by computer graphics. Users can intervene in computer models through graphic user interface. However, computer models cannot be touched in reality. If one could make a real solid model by oneself, one could understand more clearly how it would be generated and how it would be functioned. Therefore, Origami models for the alveolar duct nearly equivalent to the computer model are added, too.

The application software is named "*Lung CataChiCalaCli-er*", alias "*Lung4Cer*". Conceptual details are described in Appendix. *Lung4Cer* has been developed with VC++ by Microsoft Inc. Expected personal computers for executing the application are Windows Xp, Vista, and 7 (either 32 or 64 bit) with memory beyond 1GB. A free application software, *ParaView*, is expected to use for visualizing the models. *ParaView* is easily obtained by internet. The executing file and three manuals for *Lung4Cer*, *ParaView*, and the Origami models can be downloaded from the present author's personal homepage (http://www7b.biglobe.ne.jp/∼lung4cer/).

In the present paper, the basic construction of the software will be explained first. Next, examples of lung models generated by the software will be introduced. Finally, several problems in the software which should be improved will be discussed.

2. Basic Construction of *Lung4Cer*

2.1 Basic concepts for model generation

The human lung consists of the airway tree arising from the trachea down to the last respiratory bronchioles and the lung parenchyma containing several hundred millions of alveoli. Figure 1 indicates a simple scheme of the human lung structure. The trachea is a long duct below the vocal cords and bifurcates into right and left bronchi. These two bronchi go into the lungs, and branch about twenty times. There are no loops in the airway tree, and there is one-to-

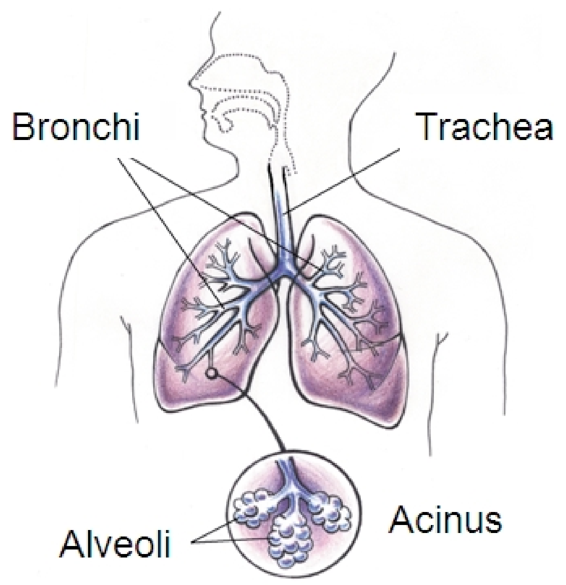

Fig. 1. Anatomical scheme of the human lung.

one correspondence between a branch and its air-supplying region in the lung.

The pulmonary acinus is defined as a parenchymal region supplied air by a terminal bronchiole (TB), and is regarded as a respiratory unit of the lung parenchyma (Weibel, 1963). The term of "bronchiole" means "a small bronchus". The TB branches three times in average and branched bronchioles are called "respiratory bronchioles (RB)" because there are a few alveolar opening in their inner walls. The last RB still branches several times, however, branched ducts are no more bronchioles but called "alveolar ducts" because the duct walls are completely replaced by alveoli (Weibel, 1963), as shown in a circle in Fig. 1. Terminal alveolar ducts with dead ends are called alveolar sacs. The subacinus, defined as the parenchymal region supplied air by the last RB, purely consists of the alveolar system without airway components (Haefeli-Bleuer and Weibel, 1998). Therefore, in this paper, not the acinus but the subacinus is used as the minimum respiratory unit. The inner structure of the subacinus is generated by two algorithms (Kitaoka *et al.*, 2000, 2007). The 3D labyrinthine algorithm assigns the air pathway in a given space (Kitaoka *et al.*, 2000), and the morphogenesis-based alveolar deformation algorithm assigns 4D structure of the alveolar duct (Kitaoka *et al.*, 2007). Although there are several other alveolar models (Weibel, 1963; Fung, 1988; Fichele *et al.*, 2004), those models do not include temporal changes. The whole lung motion is computed according to the formula in the previous paper (Kitaoka and Kawase, 2007).

Potentially, *Lung4Cer* can make a whole airway tree model with several hundred million alveoli. However, it requires incredibly huge amount of computer resource. Instead, it is feasible to select a model type according to user's interest and available computer resource. Model types provided by *Lung4Cer* are: (1) airway tree only, (2) airway tree with air-supplying parenchymal regions, (3) air pathway from the trachea to a subacinus with alveolar structure, and (4) alveolar system only.

2.2 Operation of *Lung4Cer*

The lung model generation is executed by assigning twelve parameters. "Model type" assigns a basic model type mentioned above. "Branch number in the airway tree" assigns the anatomical hierarchic level of terminal branches in the airway tree. "Region of interest (ROI)" assigns a target region for modeling, from the whole lung down to respective lung segments. There are five parameters for assigning composition of the alveolar system (details are described in the manual).

There are four parameters to assign breathing mode, lung capacities at the beginning and the end of inspiration, the ratio of inspiratory period to the total respiratory period, and the body posture. The lung capacity (LC) can be expressed by an equation as follows,

$$\mathrm{LC} = \mathrm{RV} + f \cdot \mathrm{VC},$$

where RV is the residual volume (=minimum lung volume), VC is the vital capacity (=the difference between minimum and maximum lung volumes), and f is the volume fraction of VC. LC is equal to the total lung capacity (TLC, =maximum lung volume) when $f = 1$, and is equal to RV when $f = 0$. In the present model, the functional residual capacity (FRC, =the expiratory lung volume at rest) is assigned at $f = 0.35$, and the inspiratory lung volume at rest is assigned at $f = 0.5$. Since the lung parenchymal volume is dependent on the parenchymal position and body posture, the value of f should be regarded as an approximated value rather than the absolute value. For the model type of alveolar system only, $f = 1$ indicates the maximum volume of the alveolar duct and $f = 0$ indicates the minimum value (about 20% of the maximum volume in the present algorithm).

After assignment of necessary parameters for model generation, a set of files for visualization is generated. All models indicated in the present paper are generated within ten minutes using a common PC (for example, single core of 3.3 GHz CPU with 2GB memory).

2.3 Observation of the model by "*ParaView*"

ParaView is one of the most popular free applications for scientific visualization developed in the US, which can easily be downloaded by internet. It visualizes various data from a simple graph to complex mechanical simulation data. A user can observe an object translucently, rotated, magnified, clipped, sliced, and animated. All pictures presented in the present paper were taken by *Paraview*. Basic methods for observing 4D lung models are described in the manual on the present author's homepage (http://www7b.biglobe.ne.jp/∼lung4cer/4CerManualE.pdf)

3. Examples of 4D Lung Model

3.1 Airway tree model with air-supplied parenchymal regions

A lung parenchymal region is approximated as a set of cubes whose side lengths are equal to the diameter of the air-supplying branch. There is an approximated relationship between the diameter of a branch (D) and the volume of parenchymal region to which the branch supplies air (V):

$$\mathrm{V} \simeq 1{,}000 \cdot \mathrm{D}^3.$$

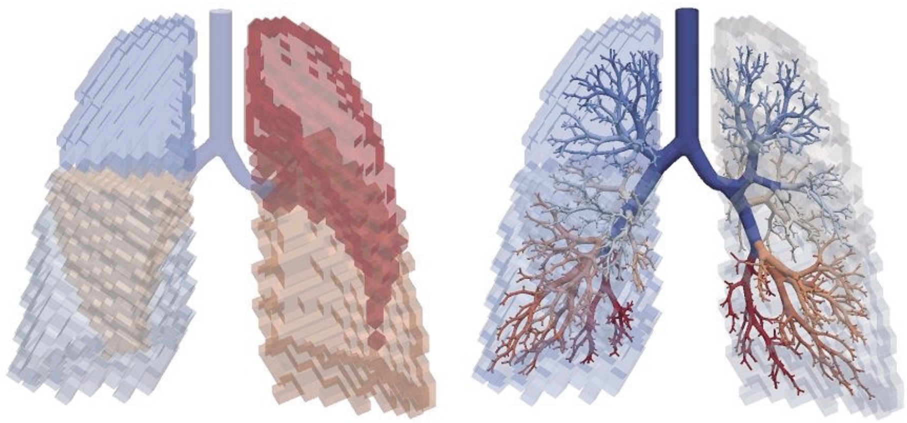

Fig. 2. Five-lobar model at TLC. Left: an airway tree down to lobar bronchi with five lobes. Right: an airway tree model of 2,921 branches is superimposed on the five-lobar model.

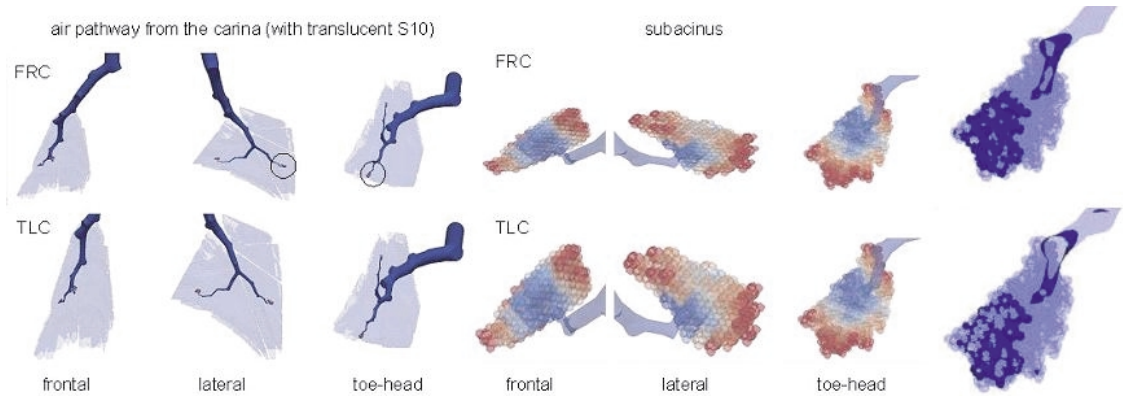

Fig. 3. Air pathway models from the trachea to two subacini. The whole region of the basal posterior segment in the right lower lobe is superimposed translucently. Magnified images in the right half are the dorsal subacinus. The right-end pictures are horizontally thin-sectioned images with 0.25 mm in thickness.

This equation indicates that each parenchymal region is approximated by a set of about 1000 cubes. To be more precise, the exponent of D is slightly smaller than 3.0 (Kitaoka *et al.*, 1999).

Figure 2 depicts a lobar bronchial tree model with five lobes. An airway tree model of 2,921 branches is superimposed in the right picture in Fig. 2. The end of each lobar bronchus is connected continuously with a cube in the lobe so that air can be moved into the lobe.

3.2 Air pathway model from the trachea to alveoli in a single subacinus

Figure 3 indicates two air pathway models from the trachea to alveoli in two subacini in the right lower lobe at upright posture. The last respiratory bronchiole (RB) located at dorsal part is the 19th generation with 0.37 mm in diameter at TLC. The right half in Fig. 3 indicates magnified views of the subacinus. Alveoli are colored by path length from the end of the last RB (red alveoli are the most distant). All alveoli are connected to the trachea through branched alveolar duct. Regional alveolar wall motion is computed by superimposing macroscopic displacement of the whole lung on the mesoscopic motion of the alveolar system. The right-end pictures in Fig. 3 indicate horizontally thin-sectioned images with 0.25 mm in thickness, mimicking clinical X-ray CT images. Net-like patterns of the alveolar wall at FRC and TLC are apparently different because of the alveolar structural change. This change causes the change in tissue density, and hence, the change in CT value. Details of the inner structure of the subacinus will be explained later.

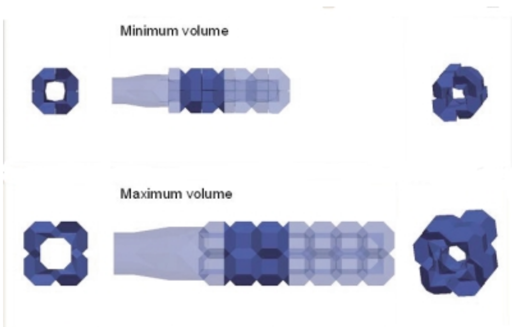

Fig. 4. A single duct unit in a straight alveolar duct model. Upper: at minimum volume. Lower: at maximum volume.

3.3 Straight alveolar duct model

Lung4Cer generates an alveolar system by connecting multiple alveolar duct units so as to make a branched space-

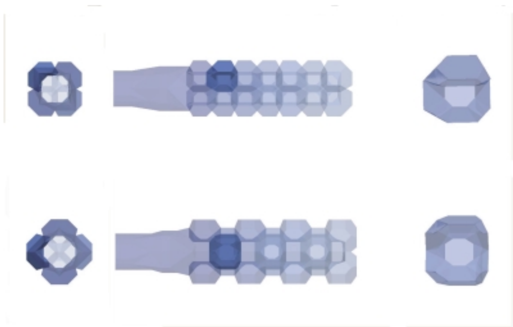

Fig. 5. A single alveolus in the straight alveolar duct model around FRC. Upper: the same view as in Fig. 4. Lower: rotated view at 45 degree around the longitudinal axis.

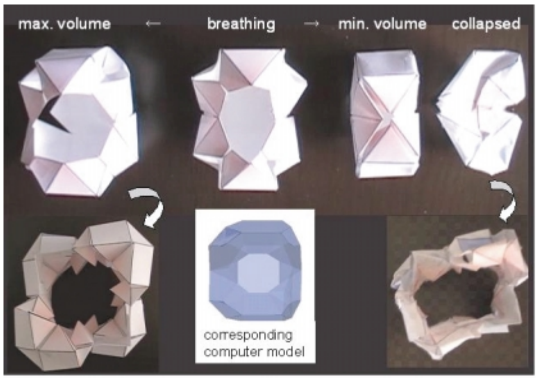

Fig. 6. Origami models for single alveolus (upper row) and alveolar duct unit (lower row). An Origami alveolus changes its shape and volume by changing folds in the mouth colored pink. An Origami alveolar duct is constructed by combining those alveoli. When all alveoli in the duct unit are collapsed, the duct unit looks as if one single alveolus had thickened alveolar wall (right end pictures).

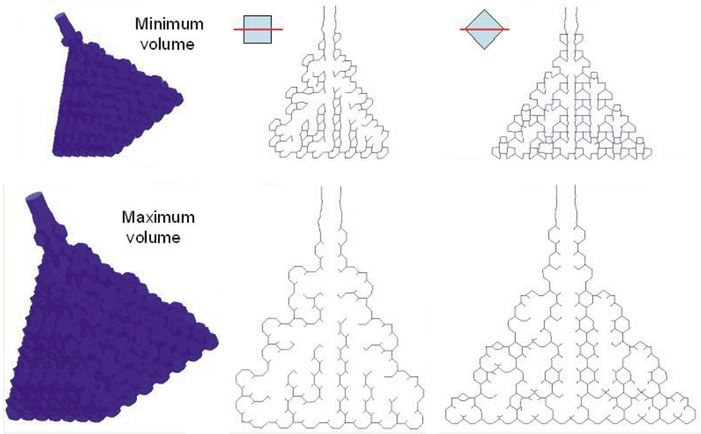

Fig. 7. Pyramid-shaped subacinar model consisting of 1,200 alveoli.

filling air pathway. A straight alveolar duct model is the minimum alveolar system in which several duct units are arranged in line. An alveolar duct unit is modeled as a deformed cubic column in which eight alveoli are contained as shown in Fig. 4. A single alveolus is a part of 18-polyhedron whose mouth is opened to the duct space as shown in Fig. 5.

The 18-polyhedron is made from a hexahedron by shaving 12 edges into hexagons, with which the face number increases from 6 to 18. The alveolar mouth shown in Fig. 5 is widened and narrowed during breathing motion as experimentally investigated in animal lungs (Mercer *et al.*, 1987; Kitaoka *et al.*, 2007). Since 80% of elastin fibers in the alveolar wall are distributed at the alveolar mouths (Mercer and Crapo, 1990), alveolar mouth is much more deformable than other part of alveolar walls (Mercer *et al.*, 1987).

The present author previously proposed simple Origami models for the alveolar system starting from square sheets (Kitaoka *et al.*, 2010). However, it was impossible to fill the space by those models. The present author has improved the Origami models so as to be nearly equivalent to the computer models, as indicated in Fig. 6. The Origami sheets and the method for making the Origami model are given in the manual (http://www7b.biglobe.ne.jp/~lung4cer/origamiManualE.pdf).

One can make and handle the model in reality. As the alveolar mouth is folded up, inner diameter of the alveolar duct become smaller, because dihedral angles between walls become smaller. When the alveolar mouth is completely folded, the mouth is closed and the alveolar duct volume reaches the minimum. One can feel the airflow on his palm while contracting the model with his both hands. Furthermore, the Origami model helps to understand the structural change in alveolar collapse as shown in Fig. 6. In the Origami model, collapsed alveolar walls are irregularly folded up as if one single wall were thickened. In addition, the open alveolar duct looks as if one single alveolus were surrounded by thickened alveolar wall. This misinterpretation is the same as the description of histologic findings of diffuse alveolar damage (DAD) in conventional textbooks (Katzenstein and Akin, 1990).

There are two different points between the computer model and the Origami model: One is that the mouth in the Origami alveolar model is not contracted but folded. However, if folding interval is very small, it behaves like an elastic sheet. The other is that all face elements in Origami model do not change their shapes but that those in the computer model slightly change shapes like an elastic membrane. Therefore, the Origami model cannot fill the space through the respiratory cycle.

3.4 Pyramidal subacinar model

Figure 7 shows a pyramid-shaped subacinar model by connecting 155 duct units. There are about 1,200 alveoli. The size, shape, and the alveolar number are nearly the same as an average human subacinus (Haefeli-Bleuer and Weibel, 1998). The approximate shape is homothetically changed during respiratory motion. Meanwhile, the internal structure is extremely nonhomothetic, as shown in cross sectional images in Fig. 7.

Right two images in each row in Fig. 7 are longitudinal cross section images at two different directions. Images at the maximum volume are similar to histologic images of normal lung tissue fixed by formalin at total lung capacity. The middle images in Fig. 7 indicate that the last RB is branched into multiple alveolar ducts which connect each other and fill the space without gap. On the contrary, there are several alveolar ducts which have no connections on the 2D slice in the left images in Fig. 7, although they are all connected in 3D. Those images teach us how difficult to estimate 3D structure from cross sectional images only. Alveolar septa protruded toward the center of duct space are cross sections of opened alveolar mouths. There are many small closed polygons and few protruded alveolar septa at the minimum volume. Those closed polygons are cross sections of alveolar space where the alveolar mouths are closed. Even though the alveolar mouths are closed, the alveolar duct space is never obstructed. These findings are consistent with histological findings recognized in rapidly-frozen sections of animal lungs at low lung volume in literatures (Young *et al.*, 1970; Robertson *et al.*, 1986).

4. Discussions and Conclusions

As long as the present author knows, it is the first to release an application software which generates 4D lung models. This kind of model generator is thought to be useful for education and research in the medical science.

There are several problems which should be overcome in the future. The first is regarding the airway tree generation. About 10% of parenchymal regions lose their air-supplying RBs because of shortcoming of the algorithm. Compared with the original code in the first publication (Kitaoka *et al.*, 1999), by which 30% of parenchymal regions lost their corresponding RBs, the improvement is thought to be enough for only visualization. However, for the purpose of precise and detailed computational mechanical simulation, further improvement is necessary.

Secondly, the alveoli in the present version are congruent each other. It is possible to generate non-congruent models as in the original paper (Kitaoka *et al.*, 2007), tough it requires considerable amount of computer resource and complicated codes. For the purpose of understanding the alveolar structure, the congruent model is thought to be sufficient. Physiological effect of irregular shapes and motions in the alveolar system should be investigated precisely in the future.

Thirdly, only gravitational ventilation inhomogeneity is taken account into breathing motion of the lung parenchyma. In order to model ventilation inhomogeneity related to unbalance of airflow and tissue elasticity, precise computation based on fluid-solid combinatory mechanics is necessary. This is one of the most important issues in ventilation mechanics both in physiological and pathological conditions. Further improvements of *Lung4Cer* will provide new insights to the ventilation inhomogeneity.

Lastly, there are no pulmonary circulation systems in the present lung models. The present author previously published a 3D lung model with pulmonary vessels (Kitaoka, 2002), although the capillary system between pulmonary arteries and veins was not included. Blood flow in the capillary bed can be parametrically modeled by the oxygen diffusion capacity as one of physicochemical properties of the alveolar wall. To incorporate the pulmonary circulation system in *Lung4Cer* is the next target to be challenged.

In conclusion, *Lung4Cer* is thought to be a powerful tool for studying respiratory anatomy and physiology towards a new paradigm of respirology.

Appendix A. CataChiCalaCli, a Novel Concept for the Structure and Function

The present author proposes a novel concept to indicate 4D structure of the living system, “CataChiCalaCli”, which are coming from Japanese words, Catachi (=form, structure) and Calacli (=machine, mechanism). Although conventional alphabetical expressions of those two words are “Katachi” and “Karakuri”, several characters are altered. “Katachi” is a composite word of “Kata” and “Chi”, meaning space and energy, respectively. “Karakuri” is also compounded of “Kara” and “Kuri”, meaning direction (or relation) and periodic time, respectively. Since “Kuri” is corresponding to “cycle” both in meaning and oral motion, its alphabetical characters are assigned so as to contain *c* and *l*. By changing *k* and *r* into *c* and *l*, respectively, a symmetric alphabetical expression, “CataChiCalaCli”, is generated.

A Japanese word, “Chicala, compounded of “Chi” and “Cala”, means “gradient vector of energy potential”, exactly the same as the definition of force in physics. When “CataChiCalaCli” is separated into “Catachi” and “Calacli”, it means geometry and kinematics, or structure and function. When it is separated into “Cata”, “Chicala”, and “Cli”, it means dynamics which connect structure and function. In addition, when “by” is inserted between “Catachi” and “Calacli”, it means the morphogenesis. Thus, “CataChiCalaCli” is thought to be an appropriate term to comprehensively indicate 4D phenomena in the living system. Since it seems impossible to translate it into English including basic four words, the present author proposes to use the Japanese original term. Hence, the present author names the application software presented in this paper “*Lung CataChiCalaCli-er*”, where the last “er” indicates a doer in English and its pronunciation also means a doer in Japanese (Ya). The present author also proposes its alias “*Lung4Cer*”, because there are four C in CataChiCalaCli. Indeed, *Lung4Cer* makes lung models in a very short time like a forcer.

References

Fichele, S., Paley, M. N. J. and Woodhouse, N. (2004) Finite-difference simulations of ^{3}He diffusion in 3D alveolar ducts, comparison with the cylinder model, *Magn. Reson. Med.*, **52**, 917–920.

Fung, Y. C. (1988) A model of the lung structure and its validation, *J. Appl. Physiol.*, **64**, 2132–2142.

Haefeli-Bleuer, B. and Weibel, E. R. (1988) Morphometry of the human pulmonary acinus, *Anat. Rec.*, **220**, 401–414.

Katzenstein, A. L. A. and Akin, F. B. (1990) Acute lung injury patterns, diffuse alveolar damage, acute interstitial pneumonia, bronchiolitis-obliterans organizing pneumonia, in *Surgical Pathology of Non-neoplastic Lung Disease* (ed. J. L. Bennington), 2nd ed., pp. 9–40, Saunders, Philadelphia.

Kitaoka, H. (2002) Computational morphology of the lung and its virtual imaging, *Euro. J. Radiol.*, **44**, 164–171.

Kitaoka, H. (2009) Breathing lung simulator from the trachea to alveoli, *48th Annual Meeting of JSBME*, P6-1-15 (in Japanese).

Kitaoka, H. and Kawase, I. (2007) A novel interpretation of closing volume based on single-breath nitrogen washout curve simulation, *J. Physiol. Sci.*, **57**, 367–376.

Kitaoka, H., Takaki, R. and Suki, B. (1999) A three-dimensional model of the human airway tree, *J. Appl. Physiol.*, **87**, 2207–2217.

Kitaoka, H., Tamura, S. and Takaki, R. (2000) A three-dimensional model of the human pulmonary acinus, *J. Appl. Physiol.*, **88**, 2260–2268.

Kitaoka, H., Nieman, G. F., Fujino, Y., Carney, D., Dirocco, J. and Kawase, I. (2007) A 4-dimensional model of the alveolar structure, *J. Physiol. Sci.*, **57**, 175–185.

Kitaoka, H., Hoyos, A. M. C. and Takaki, R. (2010) Origami model for beathing alveoli, *Adv. Expl. Med. Biol.*, **669**, 49–52.

Mercer, R. and Crapo, J. D. (1990) Spatial distribution of collagen and elastin fibers in the lungs, *J. Appl. Physiol.*, **69**, 756–765.

Mercer, R., Lacot, J. M. and Crapo, J. D. (1987) Three-dimensional reson-struction of alveoli in the rat lung for pressure-volume relationships, *J. Appl. Physiol.*, **62**, 1480–1487.

Robertson, C. H., Hall, D. L. and Hogg, J. C. (1986) A description of lung distortion due to localized pleural stress, *J. Appl. Physiol.*, **34**, 344–350.

Weibel, E. R. (1963) Volmetric composition of the lung, in *Morphometry of the Human Lung*, pp. 51–56, Academic, New York.

Young, S. L, Tierney, D. F. and Clements, J. A. (1970) Mechanism of compliance change in excised rat lungs at low transpulmonary pressure, *J. Appl. Physiol.*, **29**, 780–785.